phys. stat. sol. **35**, 237 (1969)

Subject classification: 14.4.1; 13.1; 13.4; 14.3.1; 22.9

Laboratorio di Elettronica, C.N.E.N., C.S.N. Casaccia, Roma (a), and Coordinamento Attività del C.N.E.N. nel campo dell'Elettronica e della Strumentazione, C.N.E.N., Roma (b)

Space-Charge-Limited Current and Band Structure in Amorphous Organic Films

By

G. CASERTA (a), B. RISPOLI (b), and A. SERRA (a)

Electrical conduction phenomena in thin films of some organic polymers have been investigated. The current–voltage characteristics of polymethylmetacrilate, polyvinylformal, and polyethylene-terephthalate films display a space-charge-limited current (SCLC). The steady-state SCLC and the back current are interpreted in terms of an energy band model with localized states uniformly distributed in energy within a region of the forbidden band. This region is (0.353 $\pm$ 0.025) eV wide and seems to be independent of the chemical nature of the amorphous material, the sample preparation procedure, and the sample thickness. The density per unit energy of localized states ranges from 10^{14} to 10^{18} cm^{-3} eV^{-1}.

Les caractéristiques courant–tension des films amorphes de polymethylmetacrilate, polyvinilformal et polyethyline-terephthalate montrent une conduction en présence d'une charge d'espace. Le courant de l'état stationnaire et de décharge sont interprétables par le modèle de bande d'énergie avec des niveaux localisés, uniformément répartis, en énergie, dans une région de la bande interdite. Telle région a une largeur de (0,353 $\pm$ 0,025) eV, et elle est indépendante de la nature chimique du material, de l'épaisseur du film et de la méthode de préparation des échantillons. La densité des états localisés par unité d'energie varie de 10^{14} à 10^{18} cm^{-3} eV^{-1}.

1. Introduction

The study of electrical conductivity in insulators gives a considerable amount of information on the electrical and structural characteristics of such materials and promises new solid state devices.

In insulating materials, at or below room temperature, the density of free charge carriers is extremely low and, with an electric field, non-equilibrium conditions can be achieved, which can be easily enhanced by injecting a charge through an ohmic contact. If the contact is equivalent to a sufficiently large reserve of free charges, the J–V (current density–voltage) characteristic does not depend on the manner in which the charges are generated, but is strictly connected with the charge-transport mechanism. The characteristic is generally non-linear on account of two basic causes:

the accumulation of charges between the electrodes, particularly at very high fields;

the presence of traps, within the forbidden gap, which reduce the free charge density and produce a localized charge density within the insulator.

The density, energy distribution, and nature of the traps have a determining

influence on the J–V characteristic, which also depends on the type of charges involved in the conduction process.

This paper deals with experiments carried out on three organic polymer substances: polymethylmetacrilate (PMMA), polyvinylformal (PVF), and polyethylene-terephthalate (PET). The substances were in the shape of thin films placed between two gold metal electrodes. All the samples displayed a space-charge-limited current and a uniform distribution of traps on a portion of the energy gap.

2. Theoretical Remarks

2.1 The energy band model

An important problem which arises in the study of the conductivity of insulators is that of establishing a theoretical model which is able to justify the mechanism of charge transport through the material. The latter is, very often, a polycristalline or amorphous substance or an organic polymer. The band model could seem to be inadequate to describe the electrical behaviour of such materials in which a well defined long range order is absent. This problem was discussed by Ioffe and Regel [1]. They inferred that the periodic electric field of the lattice is not essential for the occurrence of typical semiconducting properties, and the band model may be applied also in the case in which there is a loss of periodicity of the lattice.

The works of Gubanov [2] lead to the same results. However, the edges of these bands are not well defined.

Up to now the Schrödinger equation for a three-dimensional random distribution of potential has not been solved; but some qualitative generalizations have been given by Mott [3, 4]. He suggested (see also [5]) that the disordered structure may lead to some localized energy levels at the border of the bands. A critical energy E_c separates the localized states from the non-localized ones. The charge transport among the localized states can occur by tunneling, hopping, or by thermal excitation. If the energy of the carrier is greater than E_c the mean free path of carriers is great enough and the transport of carriers occurs as in a metal or crystalline semiconductor.

The localized states originated by lack of order may be considered as trapping levels similar to the localized states arising from impurities, dislocations, etc.

For the interpretation of the experimental results we shall use the band model, assuming the localized energy states uniformly distributed in energy within a range of the energy gap.

Another problem that must be solved in a theoretical model is the sign of the charge carriers injected into the film. The J–V curve allows to discriminate the electronic or hole conduction from ionic and double charge injection conduction, but does not give any information about the sign of carriers. From the theoretical point of view, the energy necessary to transfer an electron from an insulator to a metal electrode is [6]

$$E_p = I_c - \varphi \quad \text{(p-type conduction)}, \tag{1}$$

where I_c is the ionization potential of the insulator and φ the electron work function of the metal.

When the electron is transferred from the metal to the insulator the energy change is

$$E_n = \varphi - A_c \quad \text{(n-type conduction)}, \tag{2}$$

where A_c is the electron affinity of the insulator.

Depending on whether $E_p < E_n$ or $E_p > E_n$ a hole or electron injection will take place, respectively.

For most organic solids the values of the ionization potentials are about 5.5 eV [7]. Furthermore, some calculated values of electron affinities for organic amorphous polymers are about 3 eV [8]. Since in our experiments we used gold electrodes, the work function of which is 4.8 eV, from the preceding remarks it should be concluded that, in the examined polymer films, the injection of holes is more favoured than the injection of electrons.

It is possible, on the other hand, to deduce experimentally the type of the injected charges by determining, by means of electrostatic measurements, the sign of the charge trapped in the discrete energy levels.

2.2 Steady-state SCLC

Let us consider a sample of insulating material placed between two metal electrodes forming ohmic contacts with the sample. If the sample is free from traps, and if only one type of charges is injected (in our case hole injection is considered), Lampert [9] finds that the relation between current density and applied voltage is

$$J = \frac{9}{8} \mu \varepsilon \frac{V^2}{a^3} + \frac{3}{4} e \bar{n} \mu \frac{V}{a}, \tag{3}$$

where

μ mobility of the charge carriers,

ε dielectric constant of the material,

a thickness of the sample,

$\bar{n}$ density of the free charge carriers in the absence of electric field,

V voltage applied to the sample electrodes.

Equation (3) for $\bar{n} = 0$ gives the Mott and Gurney law [10]

$$J = \frac{9}{8} \mu \varepsilon \frac{V^2}{a^3}. \tag{4}$$

If traps are present, the space-charge-limited current will be reduced, since most of the injected carriers are removed by empty traps. Consequently equation (4) will be changed.

Let us consider the case in which the traps are uniformly distributed between a band edge and a cutoff energy, with the thermal equilibrium Fermi level lying in the midst of this distribution. In this case [11], after the electric field is applied, the injection of holes takes place, and the hole Fermi level moves away from the equilibrium E_F towards the valence band by an amount ΔE. It reaches a value E_F^* which depends on the total injected charge Q.

This charge can be distributed in three parts:

free charge,

trapped charge in the state below E_F^*,

trapped charge in the states between the initial Fermi level E_F and the final level E_F^*.

In order to evaluate the current density, it is necessary to know the fraction of injected charge that remains free.

The free carrier density is given by

$$n = N_v \exp\left[\frac{E_v - E_F^*}{kT}\right] = N_v \exp\left[\frac{E_v - E_F}{kT}\right] \exp\left[\frac{\Delta E}{kT}\right] = \bar{n} \exp\left[\frac{\Delta E}{kT}\right], \tag{5}$$

where N_v is the effective density of the energy level in the valence band, E_v is the edge of the valence band, and $\bar{n} = N_v \exp[(E_v - E_F)/kT]$.

As a first approximation it can be assumed that all the injected charge is trapped in the ΔE energy range. Under this assumption and the hypothesis that the traps are uniformly distributed in energy, we have

$$Q \approx \Delta E \, e \, a \, n_t^* , \tag{6}$$

where Q is the injected charge per unit area and n_t^* the density of traps per unit energy range. One assumes that

$$Q = C \, V , \tag{7}$$

where V is the applied voltage and C is the geometrical capacity per unit area of the film. This hypothesis leads to an error of a factor two at the most [9] in evaluating the trapped charge.

From (5), (6), and (7) it follows

$$n = \bar{n} \exp[\alpha \, V] , \tag{8}$$

where

$$\alpha = \frac{C}{n_t^* \, a \, e \, kT} . \tag{9}$$

Furthermore if n_t is the trapped charge density, we have

$$n_t \approx \frac{Q}{a \, e} \tag{10}$$

and therefore from (8) and (10) we obtain

$$\theta = \frac{n}{n_t} = \frac{a \, e \, \bar{n}}{V \, C} \exp[\alpha \, V] \tag{11}$$

which gives, approximately, the ratio of free to trapped charge.

The relation (4), which is valid in the absence of the traps, can be generalized by substituting the value $\mu \, \theta$ for the mobility μ, i.e. assuming that the value of mobility μ is reduced by the same factor as the number of free charges. Therefore

$$J = \frac{9}{8} \frac{\mu \, \bar{n} \, e \, \varepsilon}{a^2 \, C} V \exp[\alpha \, V] . \tag{12}$$

If the experimental characteristic complies with relation (12), it is possible to

obtain α and, through (9), the value of n_t^*. This value can also be obtained [11] disregarding equations (12) and (9).

In fact, from relations (5), (7), and (10), which disregard the energy distribution of the traps, we get

$$\theta = \frac{n}{n_t} = \frac{a\,e\,\bar{n}}{C\,V} \exp\left[\frac{\Delta E}{kT}\right]. \tag{13}$$

From (4) and (13) we obtain the general relation

$$J = R\,V \exp\left[\frac{\Delta E}{kT}\right], \tag{14}$$

where R is a constant.

From (14) we get

$$\frac{dJ}{dV} = \frac{J}{V}\left[1 + \frac{V}{kT}\frac{d(\Delta E)}{dV}\right]$$

from which

$$C\frac{d(\Delta E)}{dQ} = \left(\frac{V}{J}\frac{dJ}{dV} - 1\right)\frac{kT}{V}$$

or

$$\left(\frac{1}{e\,a}\right)\frac{dQ}{d(\Delta E)} = \left(\frac{CV}{kT}\right)\left(\frac{1}{e\,a}\right)\left[\left(\frac{V}{J}\right)\frac{dJ}{dV} - 1\right]^{-1}. \tag{15}$$

Equation (15) gives the density of traps per unit energy range.

2.3 The back current

The sample of insulating material, sandwiched between two metal electrodes, is a parallel-plate condenser. The total charge of this condenser is made up of two parts: the electrostatic charge which is localized on the plates of the condenser, and the trapped charges inside the material. If the trapped charges are uniformly distributed through the thickness of the sample, no short circuit current will flow in the external circuit (if one excepts the current transient due to compensation of the electrostatic charges on the plates). That is because, by shorting, the charges which are released from the traps are collected on both the electrodes almost in the same quantity.

The uniform distribution of trapped charge occurs when the applied field is very high, so that all the traps are occupied. Generally, after short circuit, the trapped charge density is a decreasing function of the distance from the injecting electrode. A net discharge current, associated with trap discharge, will flow in the external circuit from the injecting to the collecting electrode. In the following treatment we suppose that, after short circuit, the trapped charge distribution is strongly shifted towards the injecting electrode, so that for a convenient lapse of time the charges escaped from traps will be almost totally collected by only one electrode. As it will be shown later, the above hypothesis is confirmed by the short-circuit current measurements.

If a single trapping level is present in the gap, the probability ν_h that a hole will escape from a trap site is

$$\nu_h = \nu_0 \exp\left[-\frac{E_h}{kT}\right], \tag{16}$$

where E_h is the depth of the hole trap and ν_0 the so-called "frequency factor".

Every charge, escaped from trap, will move over a distance $\bar{l}_h$. The discharge current per unit volume will be then [12, 13]

$$i_h(t) = e\frac{\bar{l}_h}{a} n_h \nu_h \,, \tag{17}$$

where n_h is the occupation density of traps expressed by

$$n_h = n_{h0} \exp\left[-\frac{t}{\tau_h}\right]. \tag{18}$$

In (18) τ_h is the relaxation time and is equal to $1/\nu_h$.
Therefore

$$i_h(t) = e\frac{\bar{l}_h}{a}\nu_0 \, n_{h0} \exp\left[-\frac{E_h}{kT}\right]\exp\left[-\frac{t}{\tau_h}\right]. \tag{19}$$

For traps that are uniformly distributed in the energy range E_g from the valence band, a simple expression of the total discharge current may be found, provided that there is no interaction among traps.

If $i^*(t)$ is the discharge current per unit volume and per unit energy, it may be written

$$i^*(t) = e\frac{\bar{l}_0}{a}\nu_0 \, n_0^* \exp\left[-\frac{E}{kT}\right]\exp\left[-\frac{t}{\tau}\right], \tag{20}$$

where n_0^* is the occupation density per unit energy and the other symbols have the same meaning as in (19). The total discharge current is then

$$I(t) = e\frac{\bar{l}_0}{a}\nu_0 \, n_0^* \int_0^{E_g} \exp\left[-\frac{E}{kT}\right]\exp\left\{-\nu_0 \, t \exp\left[-\frac{E}{kT}\right]\right\} \mathrm{d}E \,. \tag{21}$$

By performing the integral we obtain

$$I(t) = \frac{A}{t}\left[\exp\left(-\varrho\,\nu_0\, t\right) - \exp\left(-\nu_0\, t\right)\right], \tag{22}$$

where

$$A = e\frac{\bar{l}_0}{a} n_0^* \, kT \,, \tag{23}$$

$$\varrho = \exp\left[-E_g/kT\right]. \tag{24}$$

3. Experimental Procedure

3.1 Sample preparation

The PMMA and PVF films were prepared from diluted solutions of the two polymers, respectively, in chloroform and dichloroethane. A cleaned microscope glass slide was immersed in the solutions and withdrawn after a few minutes. A film, whose thickness can be made to vary within wide limits and whose uniformity is very good, was thus obtained on the glass.

On the free face of the sample a gold layer approximately 0.01 μm thick was deposited under vacuum. The sample was then detached from the glass, and gold was deposited on the other face. Commercial grade films were used for PET.

Fig. 1. Sample mount

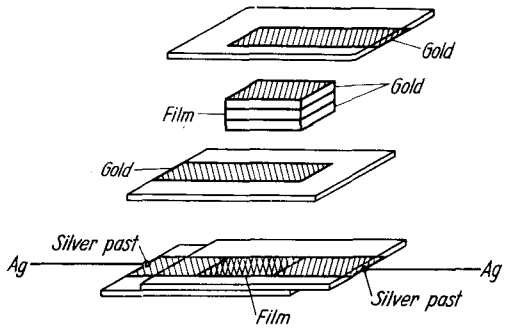

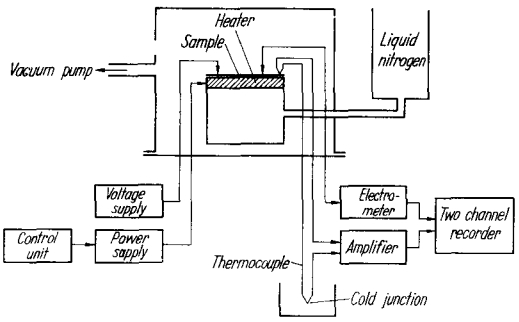

Fig. 2. Schematic diagram of the measuring apparatus

The samples thus prepared were mounted as shown in Fig. 1. The film thickness was indirectly determined by measuring the capacity of the samples. For all the said materials, the X-ray diffraction pattern showed an amorphous structure.

3.2 Measuring apparatus

Fig. 2 is a schematic diagram of the experimental apparatus used for measurements. The measurements were made keeping the sample under a vacuum of 10^{-5} Torr and at constant temperature.

The temperature of the sample, measured by a thermocouple placed in contact with the supporting glass, can be made to change continuously from 77 to 373 °K. The thermal stability of the apparatus was better than 0.5 °C. The current measurements were performed with the Keithley Mod. 610 B electrometer, with a background noise less then 10^{-14} A.

The Fluke's Mod. 408 B, with a stability better than 0.01%, was used as voltage supply.

4. Results and Discussion

4.1 The J–V characteristic

Fig. 3, 4, and 5 show the behaviour of the logarithm of conductance per unit area as a function of the applied voltage. The parameters of the straight lines were computed with the least-square method.

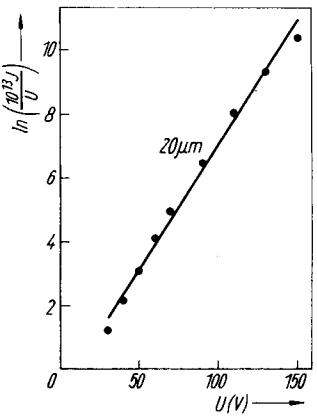

Fig. 3. Current–voltage characteristic in a ln (J/V) vs. V plot for a PVF film. $J = 0.487 \times 10^{-14}\, V \exp [0.0770\, V]$

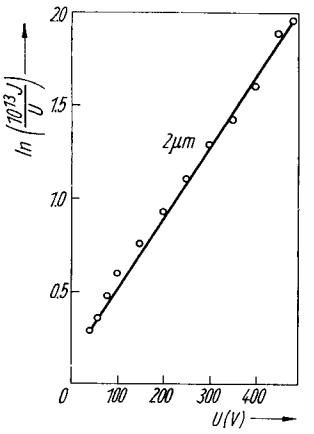

Fig. 4. Current–voltage characteristic in a ln (J/V) vs. V plot for a PET film. $J = 1.148 \times 10^{-13}\, V \times \times \exp [0.0038\, V]$

The characteristics follow the law

$$J = \text{const}\; V \exp [\beta\, V] \,, \tag{25}$$

that is of the same type as equation (12)

$$J = \left(\frac{9}{8} \frac{\varepsilon}{a^2} \frac{\mu\, e\, \bar{n}}{C} \right) V \exp [\alpha\, V]$$

which is valid for traps uniformly distributed in energy within the forbidden band.

Through equation (15), which has general validity, the value of n_t^* was calculated for different samples at different temperatures.

The values of β were calculated from the J–V characteristics. The results

Table 1

Geometrical characteristics of some polymer films and physical parameters derived from SCLC curves

Material	Thickness (μm)	Area (cm^2)	Temperature (°K)	$\beta \times 10^3$ (V^{-1})	$n_t^* \times 10^{-15}$ ($eV^{-1}\ cm^{-3}$)	$\beta\, n_t^*\, a^2\, T \times \times 10^{-10}$
PET	2	0.2	293	3.81	840	3.75
PMMA	3.8	0.2	293	481	1.57	3.19
PMMA	4.8	0.03	293	39.75	6.61	1.774
PMMA	4.8	0.03	77	45.9	24.5	1.995
PMMA	7	0.5	293	4.8	26.56	1.830
PMMA	10	0.7	293	16	3.98	1.869
PMMA	10	0.7	313	9.65	6.61	1.996
PMMA	34.5	0.65	293	2.71	1.94	1.828
PMMA	38.6	0.2	293	0.7	5.54	1.692
PMMA	47	0.2	293	0.7	3.92	1.776
PMMA	94.8	0.2	293	5.1	0.14	1.933
PVF	20	0.2	293	77.38	0.17	1.544

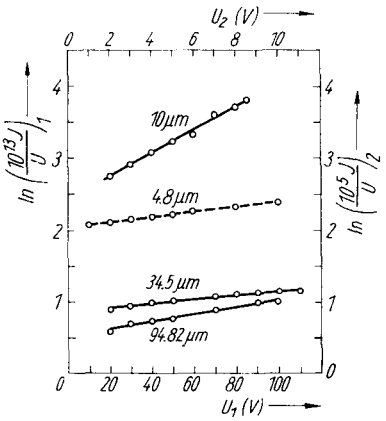

Fig. 5. Current–voltage characteristic in a $\ln(J/V)$ vs. V plot for different samples of PMMA. The dashed line is referred to $\ln_a(J/V) - V_2$-axes.
Curve A (10 μm): $J = 11.36 \times 10^{-13}\ V \exp[0.0161\ V]$.
Curve B (4.8 μm): $J = 7.81 \times 10^{-5}\ V \exp[0.0348\ V]$.
Curve C (34.5 μm): $J = 2.39 \times 10^{-13}\ V \exp[0.0027\ V]$.
Curve D (94.82 μm): $J = 1.69 \times 10^{-13}\ V \exp[0.0051\ V]$

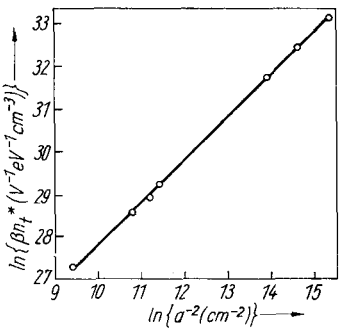

Fig. 6. Correlation between $\beta\, n_t^*$ and $1/a^2$ for PMMA films

obtained are shown in Table 1. As it can be seen, the order of the trap density per unit energy varies from 10^{14} to 10^{18}, provided that relation (6) is valid.

To check whether the coefficient β which appears in (25) had the same meaning as the coefficient α in (12), we tested if β had the same thickness and temperature dependence as α according to relation (9):

$$\alpha = \frac{\varepsilon C}{n_t^*\, a\, e\, kT} = \frac{\varepsilon \times 10^{-12}}{4\pi\, e\, kT\, n_t^*}\,\frac{1}{a^2}\,.$$

First of all, we plotted the product βn_t^* as function of $1/a^2$ for constant temperature. Fig. 6 shows $\ln(\beta n_t^*)$ as a function of $\ln(1/a^2)$ for PMMA. Similar results were obtained for the other materials. From the graph it is possible to see that there is a linear relationship between βn_t^* and $1/a^2$.

The straight line equation, which has been calculated with least-square method, is

$$\ln(\beta n_t^*) = 17.866 + \ln(1/a^2)\,. \tag{26}$$

From (26) we have $n_t^*\, a^2 = 5.85 \times 10^7$, while the theoretical value calculated from (9) is 5.95×10^7, with $\varepsilon = 3$ and $T = 293$ °K.

Furthermore, if β and α have the same temperature dependence, the product $\beta\, n_t^*\, a^2\, T$ should be constant for the same material. The last product is reported in Table 1 also. For PMMA and for thickness greater than 4 μm, the product $\beta\, n_t^*\, a^2\, T$ is approximately constant, with a standard deviation of $\pm$ 0.14. For a thickness lower than 4 μm, a discrepancy is found between the theoretical and experimental values of the above quantity. This fact is probably due to the virtual cathode near the injecting cathode, which extends into the material. The effective film thickness is, therefore, smaller than the geometrical one. The reduction of thickness is more important for very thin films than for the thicker ones. The above results clearly show that, in the examined amorphous polymers, the electrical conduction is a SCLC with traps uniformly distributed in a given energy range.

4.2 Aging effect

Fig. 7 shows the shifting of the characteristics as a function of time for PMMA. Curve A refers to the first day of measurement, curve B was plotted after three days, and curve C after four days. Curve C remains practically stable in time. Similar results have been obtained for other samples of PMMA, PVF, and PET.

In the first days of measurement the $J-V$ curve changes its slope and shifts towards an increasing conductance; after a few days only an increase of conductance occurs and a stable characteristic is gradually reached.

The observed shift can be explained if we assume that, in the aging period, a molecular rearrangement occurs and an aliquot part of the injected charges are permanently trapped. The first assumption means that the trap density varies and consequently the $J-V$ curve changes its slope; the second one justifies the increase of the conductance, because, if some traps are permanently occupied, they do not interfere in the conduction mechanism and the current density will be higher than in other cases. As border line event, if all traps were occupied, the conduction mechanism would be that of a trap-free material, with a conductance higher than in the trap-limited conduction.

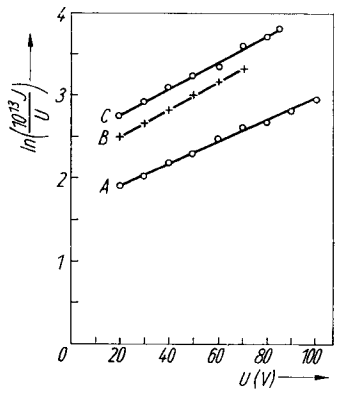

Fig. 7. Shift of the $J-V$ characteristic of PMMA films produced by aging effect

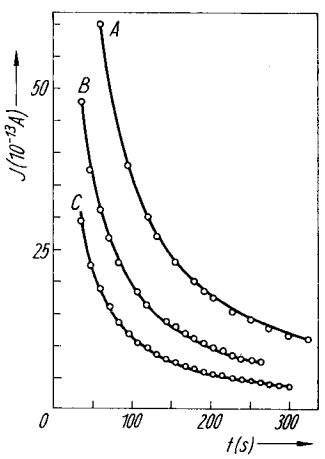

Fig. 8. Back current for a short period of time. Curve A: PMMA film 38 μm thick, curve B: PVF film 20 μm thick, curve C: PET film 2 μm thick

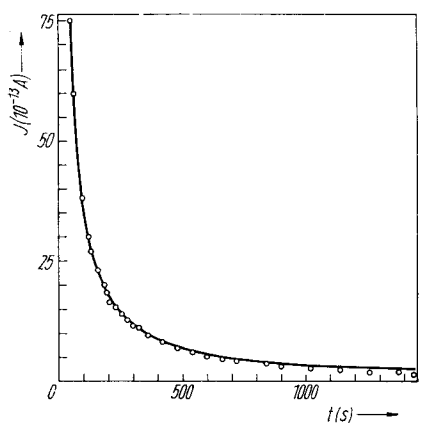

Fig. 9. Back current for a long period of time. PMMA film 38 μm thick

4.3 The back current measurements

The discharge current measurements were performed as follows:

a) After the aging time, the $J-V$ curve was traced and the SCLC region was determined;

b) for each value of the applied voltage, after the stationary current density was reached, the sample was short-circuited and the discharge current as function of time was recorded;

c) the zero time of the discharge current started a few seconds after the short circuit, in order to allow the compensation of the electrostatic charges on the electrodes. The discharge current was then only due to the charges escaped from traps.

The experimental points of the discharge curves were then fitted with equation (22), by means of the Monte Carlo method. All the calculations were performed with a IBM 7094 computer. Fig. 8 shows the very good agreement between the experimental points and the theoretical curves for a short period of time. In some cases the agreement is good for a long period of time also, as shown in Fig. 9 for PMMA film.

The last result confirms the existence of a uniform distribution of traps in a given energy range. It must be expected, however, that the validity of (22) falls down for very high values of the applied electric field, because in this case the trapped charge distribution is almost uniform inside the sample and the measured discharge current will be the difference between the charges collected on both the electrodes.

From (22) and (24) it is possible to calculate the energy range E_g in which the traps are homogeneously distributed.

In Table 2 the mean values of E_g for the three polymers are reported. For each material the mean values are calculated over a great number of discharge curves which were obtained from different experimental conditions. The value of E_g, for a given material, does not depend on the thickness of the samples or the charging voltage, and seems to be constant even when the material is changed. The mean value for all the examined materials has been calculated and was found equal to (0.353 ± 0.025) eV.

It seems, therefore, likely to suppose that the traps, which have been detected, are due to the disordered structure of the amorphous material according to Fröhlich's hypothesis [14] and Mott's treatment [3, 4].

Table 2

Mean values of the energy range in which traps are homogeneously distributed

Material	$\overline{E_g}$ (eV)
PMMA	0.340 ± 0.03
PVF	0.368 ± 0.02
PET	0.352 ± 0.01

5. Conclusions

The charge transport mechanism in three amorphous organic materials has been investigated. The experimental results can be interpreted by a theoretical model which is based on the energy band structure and localized energy levels uniformly distributed within a well-defined range of the energy gap. The same theoretical model was used by Hartke [15] for the interpretation of the conduction mechanism in amorphous selenium.

An hypothesis can be made that the examined conduction mechanism is a specific property of the amorphous materials.

Furthermore, the back current measurements have confirmed the existence of the energy range in which localized states are uniformly distributed. This energy range has, for all the samples examined in this study, the same value of 0.353 eV.

The above result leads to the conclusion that the localized energy levels are due to the lack of order of the amorphous materials rather than to impurities or dislocations.

In order to check the general validity of this supposition, measurements will be performed on different types of amorphous materials.

Acknowledgements

The authors acknowledge F. Cerquitella and E. Nicolò for their cooperation to the experiences and wish to thank Dott. L. Mango for the best fitting of the back current.

References

[1] A. F. IOFFE and A. R. REGEL, Progr. Semicond. **4**, 237 (1960).
[2] A. I. GUBANOV, Quantum Electron Theory of Amorphous Conductors, Izd. Akad. Nauk SSSR, Moscow 1963.
[3] N. F. MOTT, Adv. Phys. **17**, 49 (1967).
[4] N. F. MOTT and R. S. ALLGAIER, phys. stat. sol. **21**, 343 (1967).
[5] D. A. SEANOR, 1967 Ann. Rep., Conf. Electrical Insulation, NAS-NRC 1578 (1968) (p. 9).
[6] D. D. ELEY, J. Polymer Sci. **C17**, 73 (1967); Conf. Electrical Conduction Properties of Polymers, Pasadena 1966.
[7] L. E. LYONS, Physics and Chemistry of the Solid State, Ed. D. FOX, M. M. LABES, and A. WEISSBERGER, Interscience, 1963 (p. 746).
[8] E. SACHER, Digest of Literature on Dielectrics, National Academy of Sciences, Washington, D.C. 1967 (p. 203).
[9] M. A. LAMPERT, Phys. Rev. **103**, 1648 (1956).
[10] N. F. MOTT and R. W. GURNEY, Electronic Processes in Ionic Crystals, Oxford University Press, 1940.
[11] A. ROSE, Phys. Rev. **97**, 1538 (1955).
[12] H. BÄSSLER, G. BECKER, and N. RIEHL, phys. stat. sol. **15**, 347 (1966).
[13] C. HAMANN, phys. stat. sol. **26**, 311 (1968).
[14] H. FRÖHLICH, Proc. Roy. Soc. **A188**, 521 (1947).
[15] J. L. HARTKE, Phys. Rev. **125**, 1177 (1962).

(Received March 19, 1969)